A.

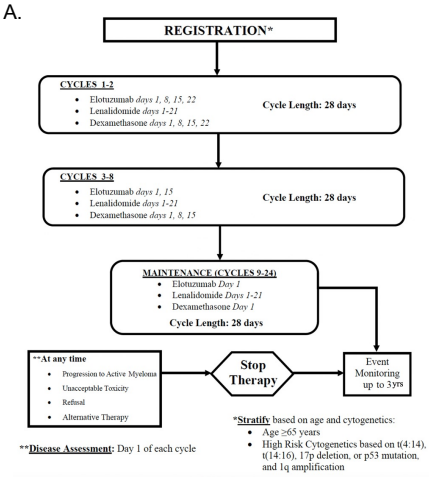

B.

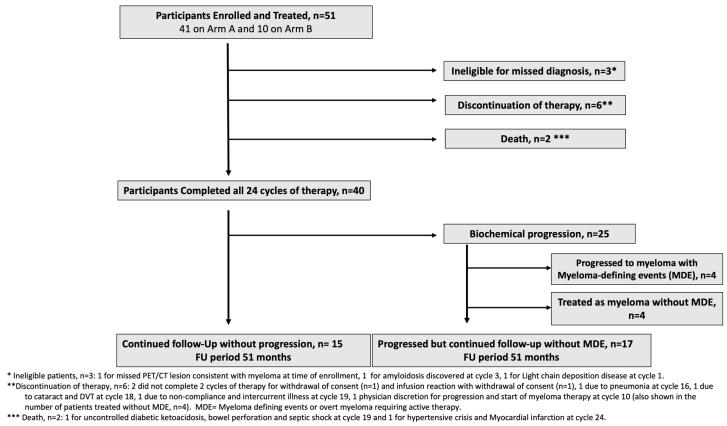

* Ineligible patients, n=3: 1 for missed PET/CT lesion consistent with myeloma at time of enrollment, 1 for amyloidosis discovered at cycle 3, 1 for Light chain deposition disease at cycle 1.
**Discontinuation of therapy, n=6: 2 did not complete 2 cycles of therapy for withdrawal of consent (n=1) and infusion reaction with withdrawal of consent (n=1), 1 due to pneumonia at cycle 16, 1 due to cataract and DVT at cycle 18, 1 due to non-compliance and intercurrent illness at cycle 19, 1 physician discretion for progression and start of myeloma therapy at cycle 10 (also shown in the number of patients treated without MDE, n=4). MDE= Myeloma defining events or overt myeloma requiring active therapy.
*** Death, n=2: 1 for uncontrolled diabetic ketoacidosis, bowel perforation and septic shock at cycle 19 and 1 for hypertensive crisis and Myocardial infarction at cycle 24.

C.

Category	Description	N=51 (%)
Hematological toxicity	Anemia	8 (16)
	Cytopenia	10 (20)
	Lymphocytopenia	14 (27)
	Lymphocytosis	1 (2)
	Neutropenia	15 (29)
	Thrombocytopenia	7 (14)
Metabolism and nutrition disorders	Diabetic ketoacidosis	1 (2)
	Hyperglycemia	12 (24)
	Hypophosphatemia	21 (41)
Infections and infestations	Lung infection	8 (16)
	Sepsis	1 (2)
	Upper respiratory infection	22 (43)
General disorders and admin site conditions	Fatigue	21 (41)
	Myocardial infarction	1 (2)
Gastrointestinal disorders	Constipation	10 (20)
	Diarrhea	10 (20)
Psychiatric disorders	Insomnia	7 (14)
Vascular disorders	Hypertension	7 (14)
Skin and subcutaneous tissue disorders	Rash maculo–papular	6 (12)
Eye disorders	Cataract	1 (2)
Hepatobiliary disorders	Cholecystitis	1 (2)

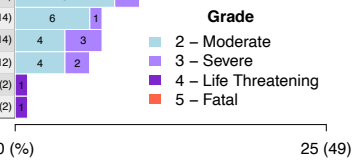

AEs grade 2+ in 10% or more of patients and all grade 4+

D.

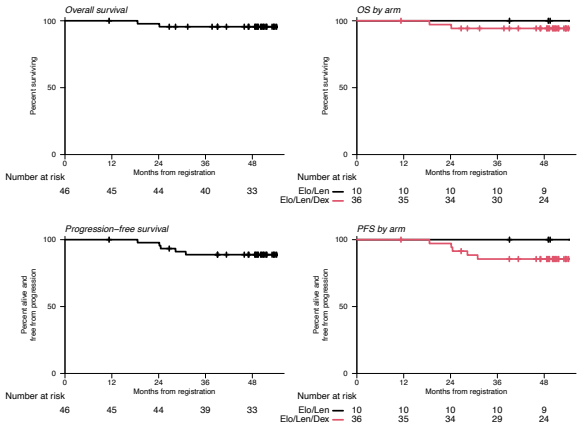

E.

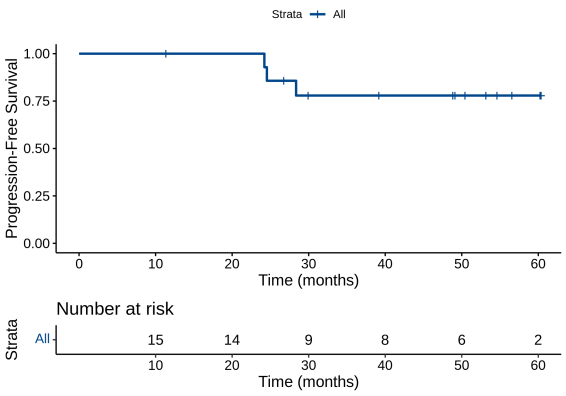

Figure S1. E-PRISM trial design and results, related to **Figure 1**. (A) E-PRISM trial schema. (B) CONSORT diagram of the E-PRISM study. (C) Treatment-related Grade 2 adverse events with at least 10% frequency and all Grade 3-5 events. (D) Kaplan-Meier curves for Overall Survival (OS) and Progression-Free Survival (PFS) in the E-PRISM cohort and by arm. (E) Kaplan-Meier curve of Progression-Free Survival (PFS) in patients from the E-PRISM cohort who were classified as high-risk based on the “20-2-20” criteria.

Table S1: Best overall response, R/N, % (90% CI), overall and by treatment arm (A: EloLenDex, B: LenDex), related to **Figure 1**.

	Evaluation					Outcome (90% CI)		
	sCR	**CR**	**VGPR**	**PR**	**MR**	**CR or better**	**VGPR or better**	**PR or better**
Treatment arm								
A:	1/36, 3% (0 - 13%)	1/36, 3% (0 - 13%)	10/36, 28% (16 - 43%)	20/36, 56% (41 - 70%)	4/36, 11% (4 - 24%)	2/36, 6% (1 - 16%)	12/36, 33% (20 - 48%)	32/36, 89% (76 - 96%)
B:	2/10, 20% (4 - 51%)	0/10, 0% (0 - 26%)	4/10, 40% (15 - 70%)	2/10, 20% (4 - 51%)	2/10, 20% (4 - 51%)	2/10, 20% (4 - 51%)	6/10, 60% (30 - 85%)	8/10, 80% (49 - 96%)
A+B	3/46, 7% (2 - 16%)	1/46, 2% (0 - 10%)	14/46, 30% (19 - 43%)	22/46, 48% (35 - 61%)	6/46, 13% (6 - 24%)	4/46, 9% (3 - 19%)	18/46, 39% (27 - 52%)	40/46, 87% (76 - 94%)

A.

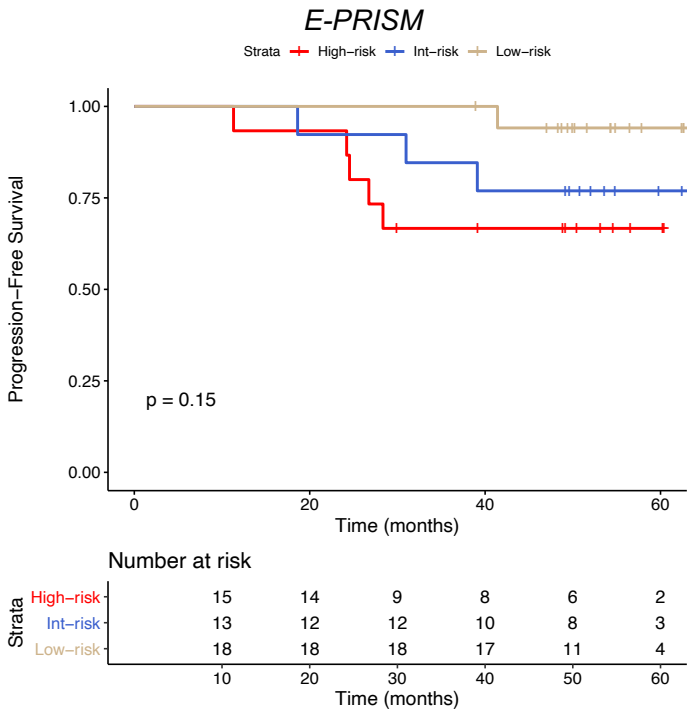
E-PRISM
Strata High−risk Int−risk Low−risk
Progression−Free Survival
1.00
0.75
0.50
0.25
0.00
p = 0.15
0
20
40
60
Time (months)
Number at risk
Strata
High−risk 15 14 9 8 6 2
Int−risk 13 12 12 10 8 3
Low−risk 18 18 18 17 11 4
10 20 30 40 50 60
Time (months)

B.

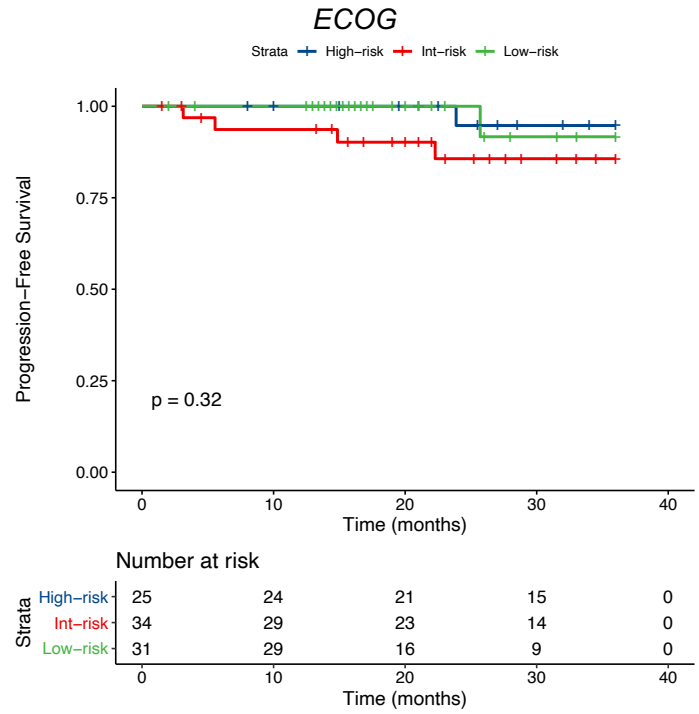
ECOG
Strata High−risk Int−risk Low−risk
Progression−Free Survival
1.00
0.75
0.50
0.25
0.00
p = 0.32
0
10
20
30
40
Time (months)
Number at risk
Strata
High−risk 25 24 21 15 0
Int−risk 34 29 23 14 0
Low−risk 31 29 16 9 0
0 10 20 30 40
Time (months)

Figure S2. Impact of “20-2-20” risk stratification on response to therapy, related to **Figure 1**. (A) Kaplan-Meier curve of Progression-Free Survival (PFS) in the E-PRISM cohort, stratified based on the “20-2-20” criteria. (B) Kaplan-Meier curve of Progression-Free Survival (PFS) in the Lenalidomide arm of the ECOG cohort, stratified based on the “20-2-20” criteria.

A.

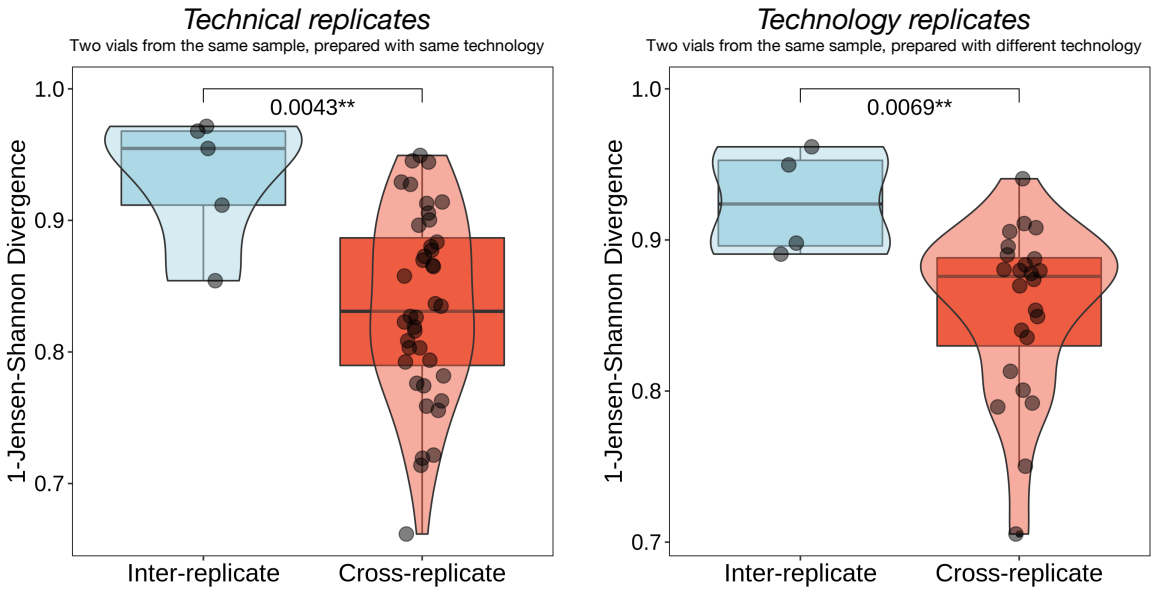
Technical replicates
Two vials from the same sample, prepared with same technology
0.0043**
1-Jensen-Shannon Divergence
1.0
0.9
0.8
0.7
Inter-replicate
Cross-replicate
Technology replicates
Two vials from the same sample, prepared with different technology
0.0069**
1-Jensen-Shannon Divergence
1.0
0.9
0.8
0.7
Inter-replicate
Cross-replicate

B.

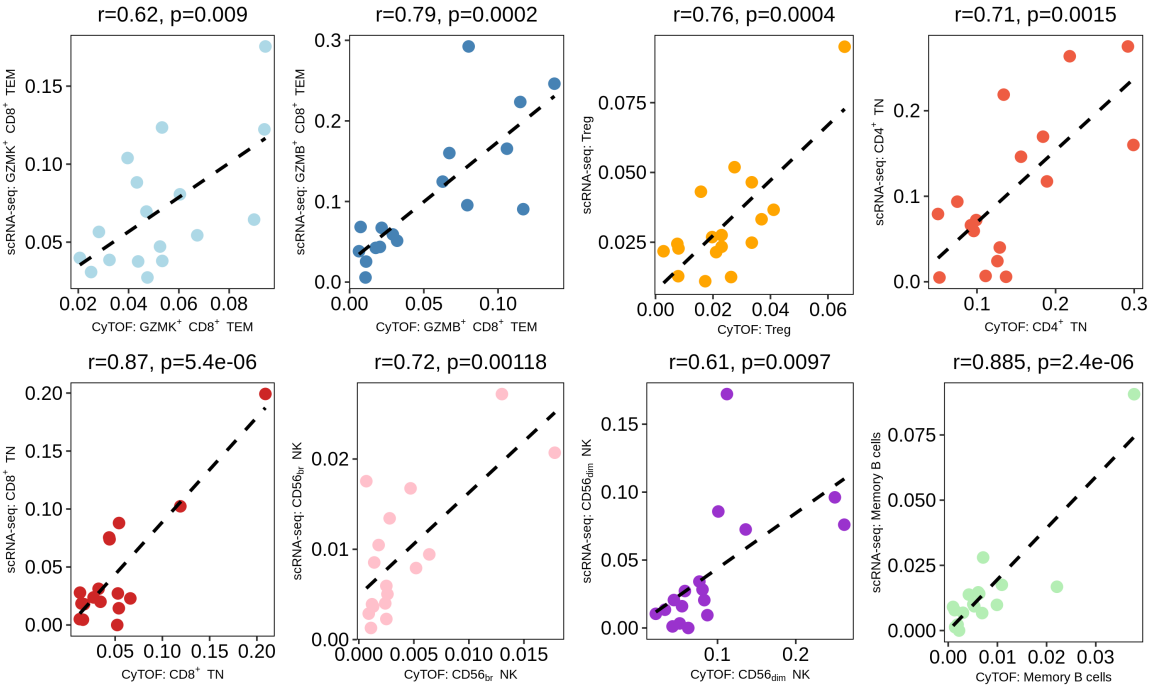
r=0.62, p=0.009
scRNA-seq: GZMK+ CD8+ TEM
CyTOF: GZMK+ CD8+ TEM
r=0.79, p=0.0002
scRNA-seq: GZMB+ CD8+ TEM
CyTOF: GZMB+ CD8+ TEM
r=0.76, p=0.0004
scRNA-seq: Treg
CyTOF: Treg
r=0.71, p=0.0015
scRNA-seq: CD4+ TN
CyTOF: CD4+ TN
r=0.87, p=5.4e-06
scRNA-seq: CD8+ TN
CyTOF: CD8+ TN
r=0.72, p=0.00118
scRNA-seq: CD56br NK
CyTOF: CD56br NK
r=0.61, p=0.0097
scRNA-seq: CD56dim NK
CyTOF: CD56dim NK
r=0.885, p=2.4e-06
scRNA-seq: Memory B cells
CyTOF: Memory B cells

Figure S3. Reproducibility of cell type abundance quantification by single-cell RNA-sequencing, related to **Figure 3**. (A) Boxplots, violin plots, and scatter plots comparing the inter-replicate Jensen-Shannon divergence of immune cell composition, compared to cross-replicate estimates for technical replicates (i.e., two cell vials from the same sample were thawed and libraries were prepared using the same technology), and technology replicates (i.e., two cell vials from the same sample were thawed and libraries were prepared using different technology for each replicate: 3'-end or 5'-end library preparation). Violin outline width represents density. P-values were computed using Wilcoxon's rank-sum test. (Box: 1st quartile, median, 3rd quartile; whiskers: +/- 1.5*IQR). (B) Scatterplots of cell type proportions as measured by single-cell RNA-sequencing (y-axis) or CyTOF (x-axis) performed on $CD138^-$ bone marrow immune cells (*n*=17). Dashed black lines correspond to the diagonal (y=x); correlation coefficients and p-values were computed with Pearson's approach.

A.

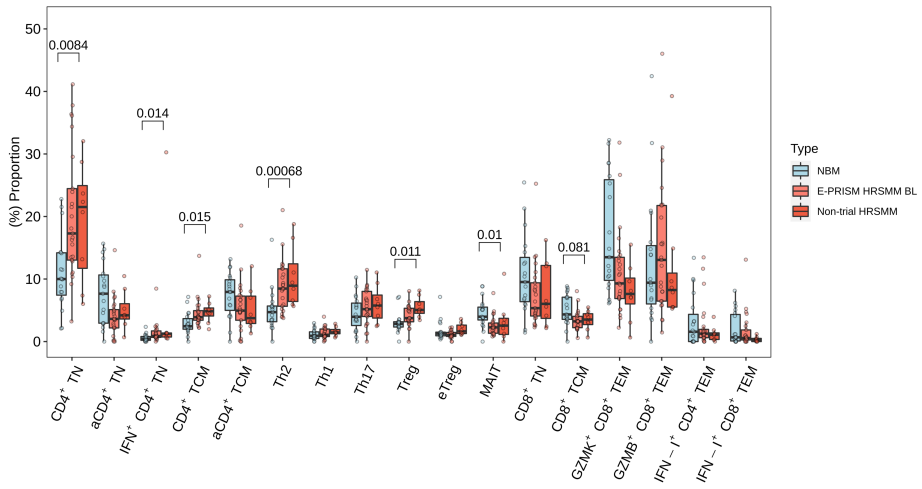
(%) Proportion
0.0084
0.014
0.015
0.00068
0.011
0.01
0.081
CD4+ TN
aCD4+ TN
IFN+ CD4+ TN
CD4+ TCM
aCD4+ TCM
Th2
Th1
Th17
Treg
eTreg
MAIT
CD8+ TN
CD8+ TCM
GZMK+ CD8+ TEM
GZMB+ CD8+ TEM
IFN − I+ CD4+ TEM
IFN − I+ CD8+ TEM
Type
NBM
E-PRISM HRSMM BL
Non-trial HRSMM

B.

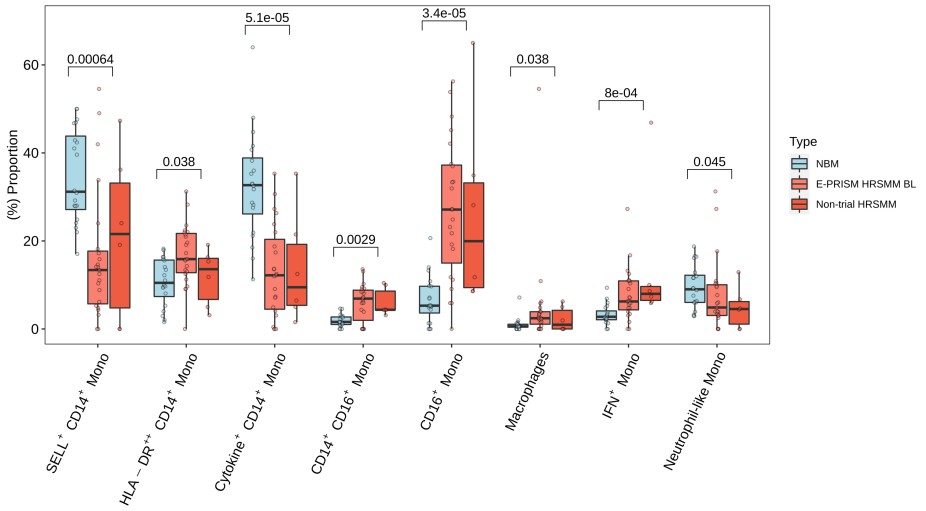
(%) Proportion
0.00064
0.038
5.1e-05
0.0029
3.4e-05
0.038
8e-04
0.045
SELL+ CD14+ Mono
HLA − DR++ CD14+ Mono
Cytokine+ CD14+ Mono
CD14+ CD16+ Mono
CD16+ Mono
Macrophages
IFN+ Mono
Neutrophil-like Mono
Type
NBM
E-PRISM HRSMM BL
Non-trial HRSMM

C.

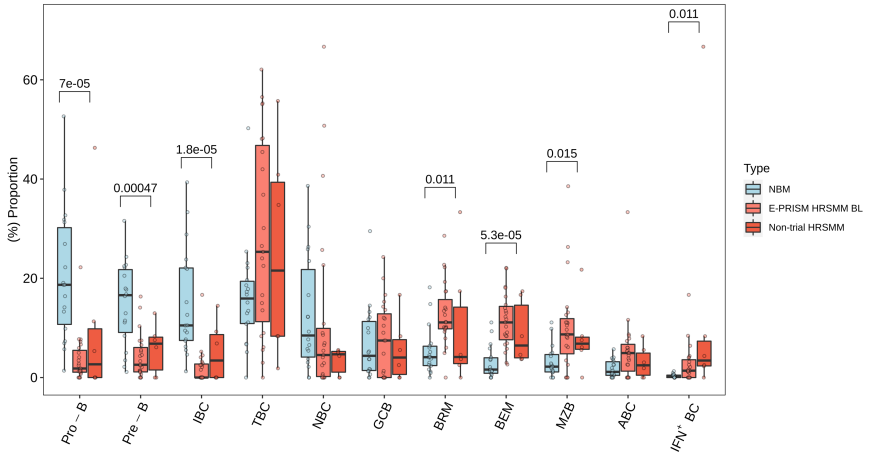
(%) Proportion
7e-05
0.00047
1.8e-05
0.011
5.3e-05
0.015
0.011
Pro − B
Pre − B
IBC
TBC
NBC
GCB
BRM
BEM
MZB
ABC
IFN+ BC
Type
NBM
E-PRISM HRSMM BL
Non-trial HRSMM

Figure S4. Alterations in BM immune cell composition in patients with HRSMM, related to **Figure 3**. Boxplots and scatterplots of (A) T cell, (B) Monocyte, and (C) B cell proportions in healthy individuals (NBM, *n*=22), patients with HRSMM in the E-PRISM cohort (*n*=26), and non-trial patients with HRSMM (*n*=9). The horizontal black line corresponds to the median, the box's hinges correspond to the first and third quartiles, the whiskers extend to the largest value within 1.5 times the interquartile range, and outliers are visualized with dots past the whisker ends. P-values were computed with Wilcoxon's rank-sum test and corrected using the Benjamini-Hochberg approach. Cell types with adjusted p-values < 0.1 have been annotated with brackets and their corresponding adjusted p-value.

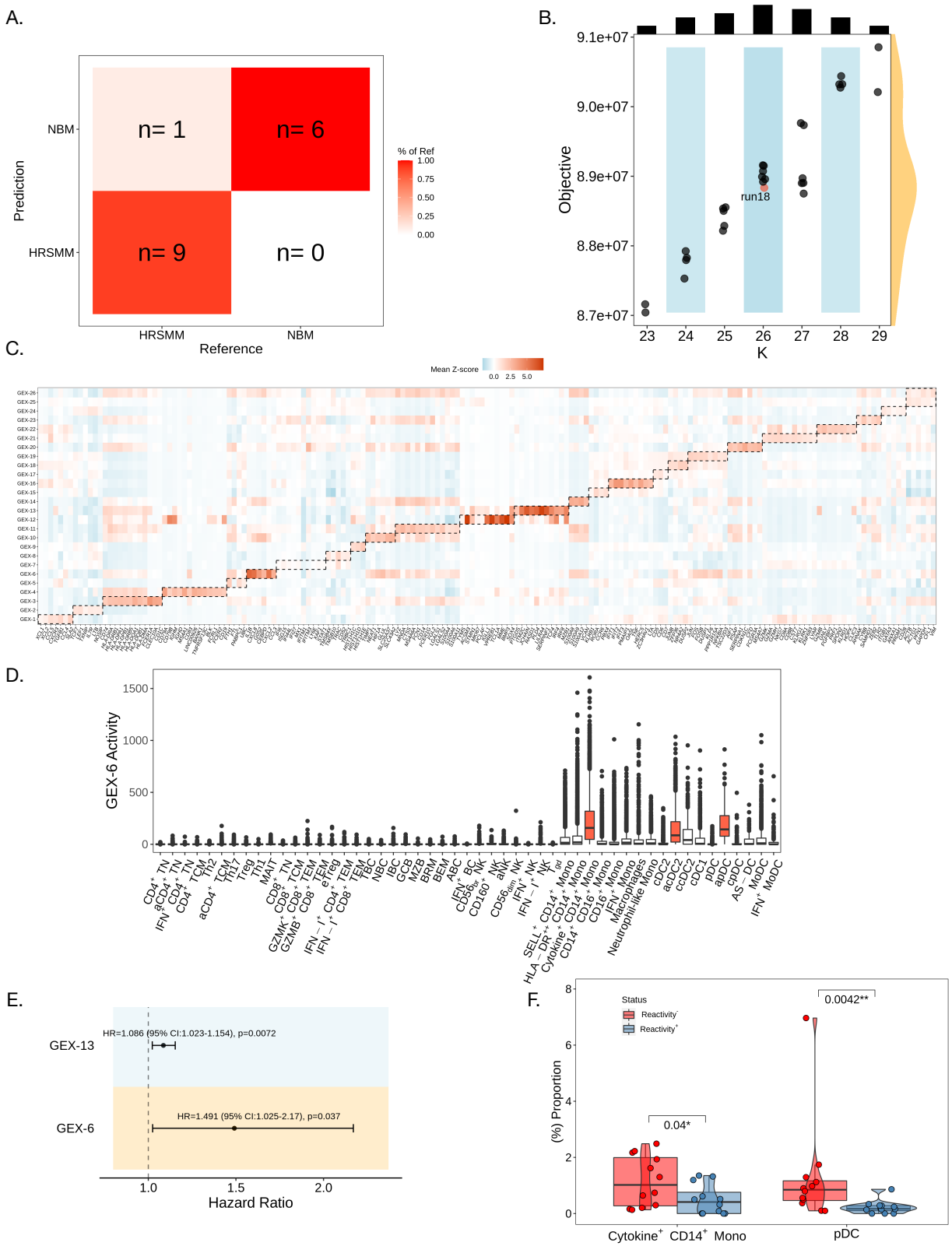
A.
NBM
HRSMM
Prediction
n= 1
n= 6
n= 9
n= 0
HRSMM
NBM
Reference
% of Ref
1.00
0.75
0.50
0.25
0.00
B.
9.1e+07
9.0e+07
8.9e+07
8.8e+07
8.7e+07
Objective
run18
23
24
25
26
27
28
29
K
C.
Mean Z-score
0.0
2.5
5.0
D.
GEX-6 Activity
1500
1000
500
0
CD4+ TN
IFN+CD4+ TN
CD4+ TN
CD4+ TCM
aCD4+ TCM
Th2
Th17
Treg
Tfh
MAIT
CD8+ TN
CD8+ TCM
CD8+ TEM
eTreg
CD4+ TEM
CD8+ TEM
TEMRA
NBC
IBC
GCB
MZB
BRM
BEM
ABC
IFN− BC
CD56bri NK
CD160+ NK
CD56dim NK
aNK
IFN+ NK
IFN− I+ NK
Tgd
SELL+ CD14+ Mono
HLA−DR++ CD14+ Mono
Cytokine+ CD14+ Mono
CD14+ Mono
CD16+ Mono
IFN+ Mono
Macrophages
Neutrophil-like Mono
cDC2
acDC2
cDC2
cDC1
pDC
apDC
cpDC
AS−DC
MoDC
IFN+ MoDC
E.
GEX-13
GEX-6
HR=1.086 (95% CI:1.023-1.154), p=0.0072
HR=1.491 (95% CI:1.025-2.17), p=0.037
1.0
1.5
2.0
Hazard Ratio
F.
Status
Reactivity−
Reactivity+
0.04*
0.0042**
(%) Proportion
8
6
4
2
0
Cytokine+ CD14+ Mono
pDC

Figure S5. Immune cell classifier and gene expression signature analysis, related to **Figure 4**. (A) Confusion matrix visualizing the performance of the disease classifier on a testing set of BM samples from patients and HD (n=16). (B) Scatterplot of the number of signatures extracted (K, x-axis) and the corresponding value of the objective function (y-axis) for each of the NMF runs (n=30). On the top axis, a histogram of the frequency of runs supporting a given K is visualized in black (mode=26). On the right axis, a density plot of the objective function values across all runs is visualized in yellow. The selected run, which has the lowest objective among runs with K equal to the distribution's mode (i.e., K=26), is highlighted in red. (C) Heatmap of mean z-scored gene expression (GEX) signature activity in cells assigned to those signatures through NMF. (D) Boxplots visualizing the activity of gene expression signature GEX-6 across lymphocytes and antigen-presenting cells. Cell types with significant activity are denoted in red. The horizontal black line corresponds to the median, the box's hinges correspond to the first and third quartiles, the whiskers extend to the largest value within 1.5 times the interquartile range, and outliers are visualized with dots past the whisker ends. (E) Forest plot showing the effect of mean BL GEX-6 and GEX-13 signature activity in the BM on PFS. Hazard ratio, 95% confidence interval, and p-value were computed using Cox proportional hazards regression. (F) Boxplots, violin plots, and scatter plots comparing the abundance of Cytokine^{+} CD14^{+} Monocytes and pDCs between patients classified as reactive (n=12) or not (n=12). Violin outline width represents density. P-values were computed with Wilcoxon's rank-sum test. (Box: 1st quartile, median, 3rd quartile; whiskers: +/- 1.5*IQR).

A.

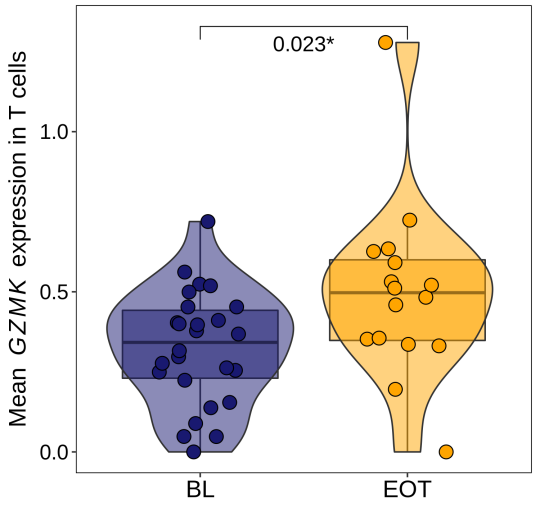
0.023*
Mean GZMK expression in T cells
1.0
0.5
0.0
BL
EOT

B.

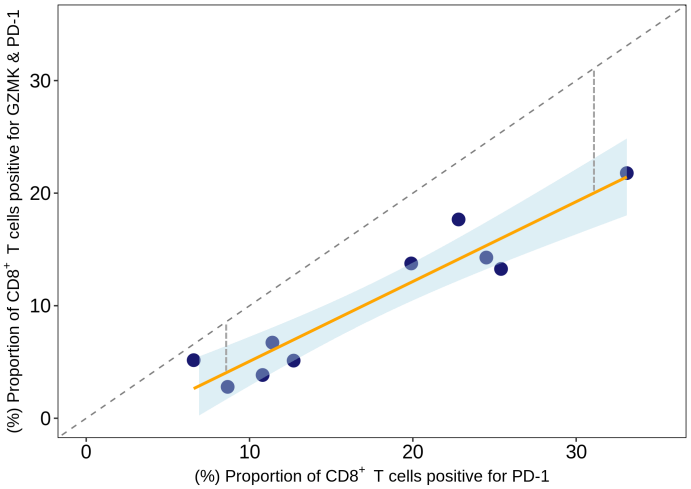
(%) Proportion of CD8+ T cells positive for GZMK & PD-1
30
20
10
0
0
10
20
30
(%) Proportion of CD8+ T cells positive for PD-1

C.

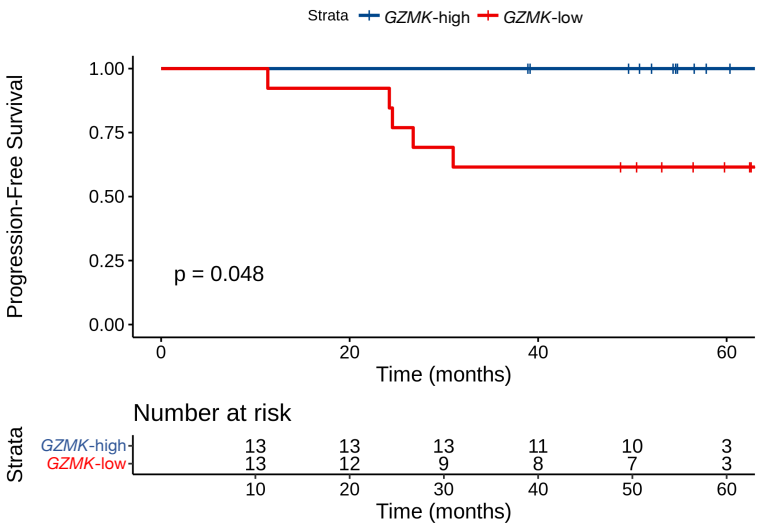
Strata
GZMK-high
GZMK-low
Progression-Free Survival
1.00
0.75
0.50
0.25
0.00
p = 0.048
0
20
40
60
Time (months)
Number at risk
Strata
GZMK-high
GZMK-low
13
13
10
13
12
20
13
9
30
11
8
40
10
7
50
3
3
60
Time (months)

Figure S6. Granzyme K-expressing $CD8^+$ TEM cells are associated with response to therapy, related to **Figure 5**. (A) Boxplots, violin plots, and scatter plots comparing mean *GZMK* expression levels in T cells of untreated patients (BL) compared to patients at EOT. Violin outline width represents density. The p-value was computed using Wilcoxon's rank-sum test. (Box: 1st quartile, median, 3rd quartile; whiskers: +/- 1.5*IQR). (B) Scatterplot of the proportion of $CD8^+$ T cells that were positive for PD-1 (x-axis), and the proportion of $CD8^+$ T cells and were positive for both PD-1 and GZMK (y-axis) by CyTOF. A regression line is visualized (in orange), together with its standard error (in light blue). The dashed grey lines correspond to the diagonal (y=x) and the vertical distances from the regression line to the diagonal. (C) Kaplan-Meier curve of progression-free survival in the E-PRISM cohort, stratified based on the mean expression of *GZMK* across all T cells.

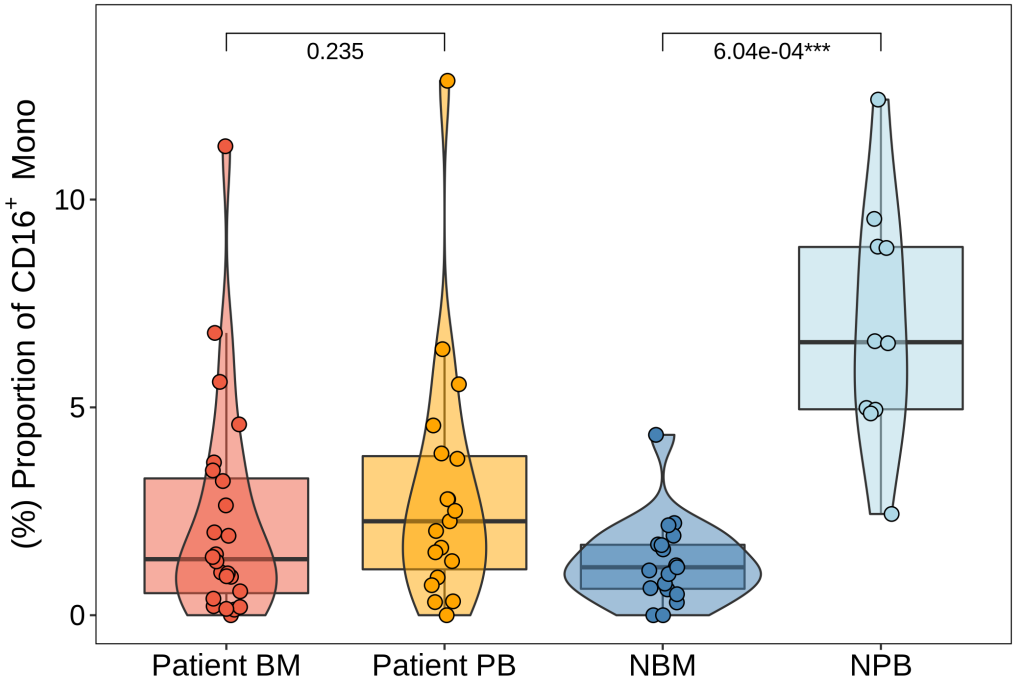
0.235
6.04e-04***
(%) Proportion of CD16+ Mono
10
5
0
Patient BM
Patient PB
NBM
NPB

Figure S7. Possible homing of $CD16^+$ monocytes to the patient BM, related to **Figure 6**. Boxplot, violin plot, and scatter plot showing the abundance of $CD16^+$ monocytes in patient BM (BM), patient PB (PB), HD BM (NBM), and HD PB (NPB). Violin outline width represents density. P-values were computed using a paired t-test for matched patient BM and PB samples, and Wilcoxon's rank-sum test for unmatched HD BM and PB samples. (Box: 1st quartile, median, 3rd quartile; whiskers: +/- 1.5*IQR).

A.

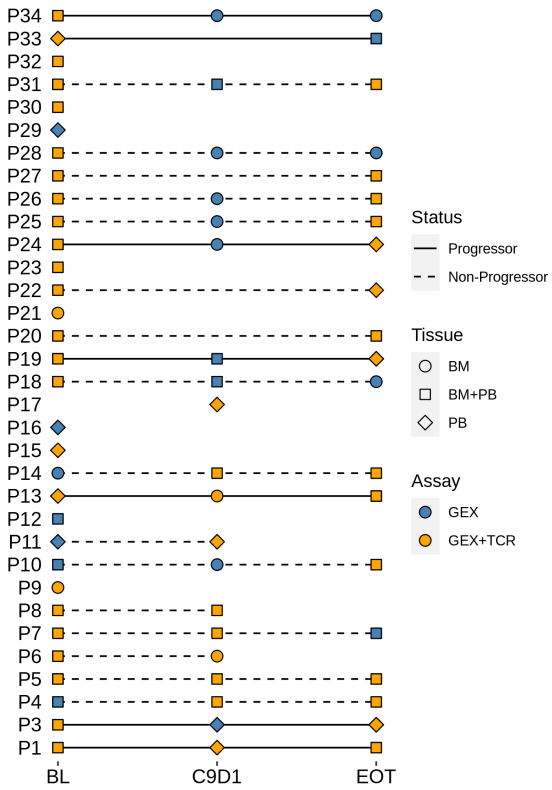
P34
P33
P32
P31
P30
P29
P28
P27
P26
P25
P24
P23
P22
P21
P20
P19
P18
P17
P16
P15
P14
P13
P12
P11
P10
P9
P8
P7
P6
P5
P4
P3
P1
BL
C9D1
EOT
Status
Progressor
Non-Progressor
Tissue
BM
BM+PB
PB
Assay
GEX
GEX+TCR

B.

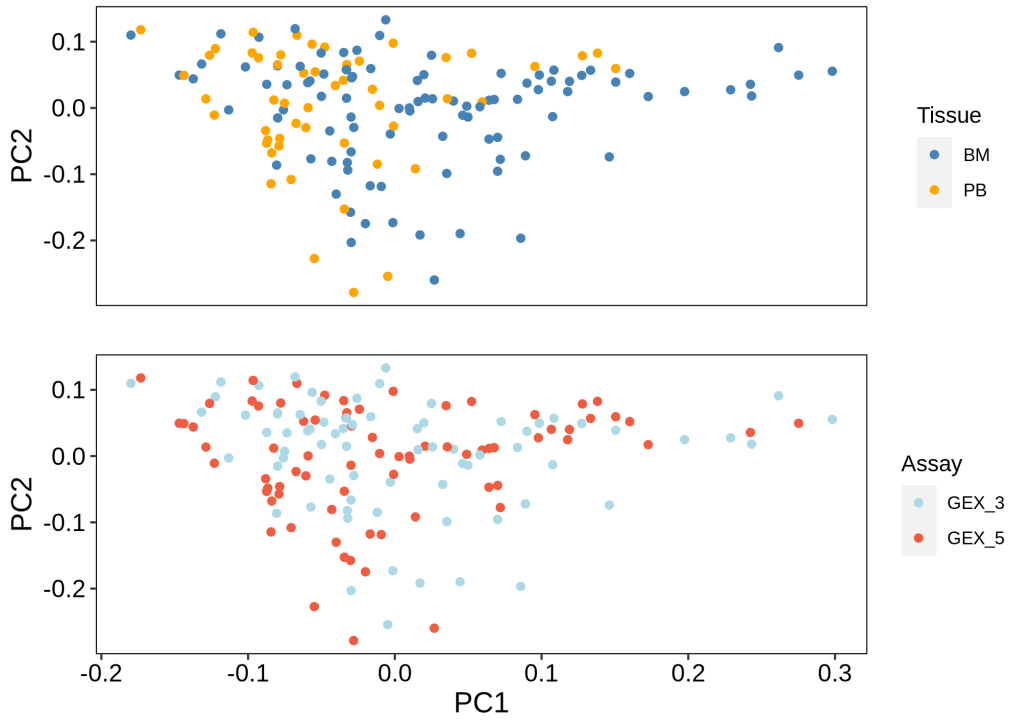
PC2
0.1
0.0
-0.1
-0.2
Tissue
BM
PB
PC2
0.1
0.0
-0.1
-0.2
Assay
GEX_3
GEX_5
-0.2
-0.1
0.0
0.1
0.2
0.3
PC1

Figure S8. Cohort diagram and dataset integration, related to **STAR Methods**. (A) Cohort diagram. (B) Scatterplot of immune cell composition principal components 1 (PC1, x axis) and 2 (PC2, y axis) demonstrating the absence of an observable batch effect due to the samples' tissue of origin or library preparation technology (n=176).